Testing for lack of fit in inverse regression – with applications to biophotonic imaging

Nicolai Bissantz[1], Gerda Claeskens[2], Hajo Holzmann[3] and Axel Munk[4]

[1]Fakultät für Mathematik
Ruhr-Universität Bochum, Germany

[2]ORStat & Leuven Statistics Research Center
K.U.Leuven, Belgium

[3]Institut für Stochastik
Universität Karlsruhe, Germany

[4]Institut für Mathematische Stochastik
Georg-August-Universität Göttingen, Germany

February 26, 2008

Abstract

We propose two test statistics for use in inverse regression problems $Y = K\theta + \epsilon$, where K is a given linear operator which cannot be continuously inverted. Thus, only noisy, indirect observations Y for the function θ are available. Both test statistics have a counterpart in classical hypothesis testing, where they are called the order selection test and the data-driven Neyman smooth test. We also introduce two model selection criteria which extend the classical AIC and BIC to inverse regression problems. In a simulation study we show that the inverse order selection and Neyman smooth tests outperform their direct counterparts in many cases. The theory is motivated by data arising in confocal fluorescence microscopy. Here, images are observed with blurring, modeled as convolution, and stochastic error at subsequent times. The aim is then to reduce the signal to noise ratio by averaging over the distinct images. In this context it is relevant to decide whether the images are still equal, or have changed by outside influences such as moving of the object table.

Keywords: Hypothesis testing, Inverse problems, Model selection, Nanoscale bioimaging, Nonparametric regression, Order selection.

1 Introduction

Statistical estimation theory for ill-posed inverse problems, particularly by nonparametric techniques, has been studied intensively within recent years. Examples which fall into this context include deconvolution problems (cf. Fan, 1991, and Johnstone et al., 2004), positron emission and X-ray tomography (Johnstone and Silverman, 1991, and Cavalier, 2000), the heat equation (Mair and Ruymgaart, 1996), imaging (Kaipio and Somersalo, 2005) or problems related to satellite gradiometry (Bissantz et al., 2007).

[1]Address for correspondence: Dr. Nicolai Bissantz, Faculty of Mathematics, Ruhr-University Bochum, Universitätsstraße 150, Mathematik III NA 3/70, D-44780 Bochum, Germany, email: nicolai.bissantz@rub.de, Phone: +49/234/32–23291, Fax: +49/234/32–14559

In these models the object of interest, i.e. the unknown density or regression function θ, is not observed directly but only after an application of an operator K, which for simplicity is assumed to be known throughout most parts of this paper. More specifically, suppose that we have observations (z_k, Y_k), $k = 1, \ldots, n$, from the model

$$Y_k = (K\theta)(z_k) + \epsilon_k, \tag{1}$$

where the z_k are fixed design points, the ϵ_k's are i.i.d. errors with $E\epsilon_k = 0$, $E\epsilon_k^2 = \sigma^2$ and $E\epsilon_k^4 < \infty$, and K is a compact injective linear integral operator between L^2–spaces $L^2(\mu_1)$ and $L^2(\mu_2)$, for measures μ_1, μ_2.

Much work focuses on optimal estimation of θ in a mean integrated square error sense, cf. Mair and Ruymgaart (1996), Cavalier and Tsybakov (2002) and Hoffmann and Reiß (2007), among many others. It is well-known that due to the ill-posedness of the problem, one obtains slower rates of convergence for estimating the unknown signal θ than for nonparametric estimates with direct observations. The actual rate of convergence is determined both by the smoothness of θ as well as by the degree of ill-posedness of the inverse problem. Roughly speaking, for so-called mildly ill-posed problems, one still has a polynomial rate of convergence, while for severely ill-posed problems (including Gaussian deconvolution), in general only logarithmic rates can be obtained. For extensive discussion see Bissantz et al. (2007).

Since nonparametric estimation of θ in inverse problems is hard, parametric modeling may become particularly interesting, whenever feasible. However, before actually employing parametric models, one should assess their adequacy via a lack-of-fit (or goodness-of-fit) test. For deconvolution density estimation, L^2-type statistics for testing goodness-of-fit are discussed in Holzmann et al. (2007). An application to parametric modeling of the brightness distribution in the Milky Way is given in Bissantz et al. (2003). Yet, to our knowledge, for inverse regression models there are no specific methods available. In this paper we shall provide such methods.

We construct omnibus tests, these are tests which are consistent against a wide class of alternative models, by extending the concept of order selection tests and Neyman smooth type tests to the setting of inverse regression models. Lack-of-fit testing based on selecting an appropriate order of an orthogonal series expansion was studied first by Eubank and Hart (1992) and was termed order selection testing, since indeed one form of the test statistic can be viewed as a test on the selected (or estimated) order of the series. Its area of application was extended from linear regression models to likelihood based models by Aerts, Claeskens and Hart (1999, 2000). The selected order in such a test is obtained via a modified version of Akaike's (1973) information criterion. A similar type of test, though originally introduced for testing the distribution function in a goodness-of-fit setting, uses instead the Bayesian information criterion (Schwarz, 1978). These tests build on the idea of a Neyman (1937) smooth test and were introduced by Ledwina (1994). Both the order selection test and the Neyman smooth test extend naturally to inverse regression modeling, where the orthogonal series expansion is canonically given by the singular value expansion, and the ordering of the singular functions is determined by the magnitude of the corresponding singular values.

In this paper we study tests for the null hypothesis that the regression function θ lies in some finite-dimensional subspace of $L^2(\mu_1)$, i.e. that

$$H_0 : \theta(z) = \sum_{j=1}^{p} a_j t_j(z), \tag{2}$$

where the t_j are given functions in $L^2(\mu_1)$. Note that since K is injective, we could equivalently rephrase the hypothesis H_0 to

$$H_0' : (K\theta)(z) = \sum_{j=1}^{p} a_j K(t_j)(z).$$

Since the integral operator K and the functions t_j are known, the hypothesis H_0' is completely specified. Further, $K\theta$ follows a direct regression model, and therefore the above mentioned methods could be applied to test H_0'. Nevertheless, there are several reasons why it is preferable to test the hypothesis H_0 directly. First, H_0 and not H_0' is the natural way to formulate the hypothesis. Second, deviations from the hypothesis H_0 might be somewhat easier to detect, since an extra application of the integral operator K typically has a smoothing effect. Thus testing H_0 directly may result in a more efficient test (cf. also Holzmann et al., 2007, for a theoretical investigation and simulation results in density deconvolution). Moreover, testing H_0 directly allows testing in situations where K is unknown (but has to be estimated as well) and where the hypothesis H_0' is therefore not completely determined.

We consider testing specific linear hypotheses, namely where the regression function is assumed to be a finite linear combination of certain singular functions, i.e. the basis functions of $L^2(\mu_1)$ occurring in the singular value decomposition of K. There are several situations where this is of particular interest. One such example is when K is self-adjoint and its eigenfunctions are trigonometric basis functions. In this case, testing the hypothesis H_0 given in (2) amounts to testing whether θ only has finitely many frequencies, where p determines the maximal frequency allowed in θ under H_0. In case of rejecting H_0, the modified order selection test will also provide an alternative estimate of the maximal frequency contained in θ.

The paper is organized as follows. In Section 2 we introduce the singular value decomposition and formulate the hypotheses that we are going to investigate. Further, we discuss examples for model (1). Section 3.1 contains a version of the order-selection test for inverse regression models, which was originally introduced for direct regression by Eubank and Hart (1992). In Section 3.2 we construct an inverse data-driven Neyman smooth test, as proposed by Ledwina (1994) for direct density testing. In a simulation study in Section 4 we investigate the power properties of our methods, as compared to tests based on the direct hypothesis H_0'. It turns out that against alternatives which contain additional eigenfunctions (or more precisely, functions from the singular value decomposition), our methods have a significantly higher power than methods based on H_0'.

Our study is motivated by a problem in fluorescence nanoscale microscopy. Here, images are observed with blurring and stochastic noise, and the aim is to detect structural changes in this sequence of images. Thus, in Section 5 we extend our methodology to test whether the distinct images observed in this deconvolution problem are equal up to possibly different intensities.

Both the order selection test and the data-driven Neyman smooth test are closely related to model selection criteria, specifically to the Akaike information criterion (AIC) and the Bayesian information criterion (BIC), and in Section 6 we discuss extensions of our procedures to model selection. All proofs are deferred to the appendix.

2 Inverse regression models

2.1 Singular value decomposition

Since K in model (1) is assumed to be compact, we can consider its singular value decomposition (cf. Kress 1999, p. 277). More precisely, there exist orthonormal bases (ϕ_j) of $L^2(\mu_1)$ and (ψ_j) of $L^2(\mu_2)$, and singular values $\lambda_j > 0$, such that $K\phi_j = \lambda_j\psi_j$ and $K^*\psi_j = \lambda_j\phi_j$. Here K^* denotes the adjoint operator of K (Kress 1999, p. 40). We shall assume that the inverse problem (1) is mildly ill-posed, so that the singular values λ_j decay polynomially. Specifically, we suppose that there exist $c, C, \beta > 0$ such that

$$c\, j^{-\beta} \leq \lambda_j \leq C\, j^{-\beta}, \quad j \geq 1. \tag{3}$$

Examples for mildly ill-posed inverse problems are given in Section 2.2. In contrast, an inverse problem is called severely ill-posed if the singular values λ_j decay exponentially fast, for which the successive theory, at least in its present form, does not apply. An example is the backward heat equation (cf. Kress 1999, p. 267).
The hypotheses that we are interested in are of the form

$$H_0 : \theta = \sum_{j=1}^{p} a_j \phi_j, \tag{4}$$

for some (fixed) p. Note that by orthogonality of the (ϕ_j), $a_j =< \theta, \phi_j >_{L^2(\mu_1)}$. The hypothesis H_0' now takes the form

$$H_0' : K\theta = \sum_{j=1}^{p} b_j \psi_j,$$

where $b_j =< K\theta, \psi_j >_{L^2(\mu_2)}$ satisfies $b_j = \lambda_j a_j$. If it is assumed that averaging over the design points z_k is close to integration w.r.t. μ_2, an estimate for b_j is given by

$$\hat{b}_{j,n} = \frac{1}{n} \sum_{k=1}^{n} \psi_j(z_k) Y_k.$$

In this paper we impose for simplicity the following

Assumption 1. Assume that

$$\frac{1}{n} \sum_{k=1}^{n} \psi_i(z_k)\psi_j(z_k) = \delta_{i,j}, \quad i, j = 1, \ldots, n,$$

with $\delta_{i,j}$ the Kronecker delta.

Under hypothesis H_0, see (4), and Assumption 1, for $j = p+1, \ldots, n$,

$$\hat{b}_{j,n} = \frac{1}{n} \sum_{k=1}^{n} \psi_j(z_k)\epsilon_k.$$

Further, $E\hat{b}_{j,n} = 0$, $E(\hat{b}_{i,n}\hat{b}_{j,n}) = \delta_{i,j}\, \sigma^2/n$, $i, j = p+1, \ldots, n$. Then an estimator for a_j is given by $\hat{a}_{j,n} = \hat{b}_{j,n}/\lambda_j$. The tests suggested in Section 3 will be based on the magnitude of the $\hat{a}_{j,n}$.

2.2 Examples

Example 1 (*Deconvolution*)**.** Suppose that $\theta, g \in L^2[0,1]$ are periodic functions, and consider the convolution operator

$$(K\theta)(z) = g * \theta(z) = \int_0^1 g(z-t)\theta(t)\,dt.$$

First consider the subspace of functions in $L^2[0,1]$ which are symmetric around $1/2$ (in the following denoted by $L^2_s[0,1]$), and suppose that $\theta, g \in L^2_s[0,1]$. The operator K is self-adjoint on $L^2_s[0,1]$, has eigenfunctions $\phi_j(t) = \sqrt{2}\cos(2(j-1)\pi t)$, $j \geq 1$, and eigenvalues

$$\lambda_j = \int_0^1 g(t)\phi_j(t)\,dt, \quad j \geq 1.$$

These are the non-zero Fourier coefficients of g. For the λ_j we assume the polynomial decay (3), which implies that g is of finite smoothness. An orthogonal design is e.g. given by the uniform design

$$z_k = (k-1/2)/n, \qquad k = 1, \ldots, n. \tag{5}$$

The hypothesis H_0 means that we test for finite frequencies in the signal θ.

If one drops the symmetry assumption on g (and on θ), the example gets more difficult, since it involves complex eigenfunctions. In fact, on the space $L^2_{\mathbb{C}}[0,1]$ of complex-valued square-integrable functions, the operator K is a normal operator for general (real-valued) $g \in L^2[0,1]$ with eigenfunctions $\phi_j(t) = \exp(2\pi i j t)$, $j \in \mathbb{Z}$, and eigenvalues

$$\lambda_j = \int_0^1 g(t)\, e^{-2\pi i j t}\,dt, \qquad j \in \mathbb{Z}.$$

Here one estimates the Fourier coefficients of $K\theta$ by

$$\hat{b}_{j,n} = \frac{1}{n}\sum_{k=1}^{n} Y_k \overline{\phi_j}(z_k),$$

where $\bar{w}$ denotes the complex conjugate of $w \in \mathbb{C}$. Since the observations Y_k and the convolution function g are real, $\lambda_j = \overline{\lambda}_{-j}$ and $\hat{b}_{j,n} = \overline{\hat{b}}_{-j,n}$. Therefore, in the test statistics introduced in Section 3, one should only use the values $|\hat{b}_{j,n}|^2$ or $|\hat{b}_{j,n}/\lambda_j|^2$ for $j > p$, in which case the theory could be developed in an analogous way.

The example generalizes easily to the two- and multidimensional case as well as to the two-sample case with equal blurring function g and design points (z_k), as considered in the application in Section 5.

Example 2 (*Radon Transform and Tomography*)**.** The Radon transform is of substantial practical importance as it describes e.g. the map of a cross-section through a patient's body onto the detector space in computer or emission tomography. For detailed information on computarized tomography see e.g. Natterer (1986). In a statistical framework, emission tomography was studied by Vardi et al. (1985), Johnstone and Silverman (1990) and Goldenshluger and Spokoiny (2006), among others.

In a simple framework, the operator in the Radon transform K_R can be represented by a

linear, injective integral operator which maps a function in the "brain space" $L^2(B, \mu_B)$ of emission densities in the patient's body to the "detector space" $L^2(D, \mu_D)$. Here B is the unit disc, parametrized by polar coordinates (r, ϑ), and D is parametrized by the angle $\varphi \in [0, 2\pi)$ of the detected line through the patient's body, and its impact parameter $s \in [-1, 1]$. The Radon operator K_R is then given by

$$K_R\theta(s,\varphi) = \frac{1}{2\sqrt{1-s^2}} \int_{-\sqrt{1-s^2}}^{\sqrt{1-s^2}} \theta\left(s\cos(\varphi) - t\sin(\varphi), s\sin(\varphi) + t\cos(\varphi)\right) dt,$$

where $\theta \in L^2(B, \mu_B)$, and $d\mu_B(r, \vartheta) = \frac{r}{\pi} dr d\vartheta$. It maps injectively into the space $L^2_{inv} \subset L^2(D, \mu_D)$ of functions on D satisfying $f(s, \varphi) = f(-s, \pi + \varphi)$, and where $d\mu_D(s, \varphi) = \frac{1}{\pi^2}(1 - s^2)^{1/2} ds d\varphi$. In brain space, the singular value decomposition involves the Zernike functions

$$\phi_{(p,q)}(r, \vartheta) = \sqrt{q+1} \cdot Z_q^{|p|} e^{ip\vartheta}, \quad q = 0, 1, 2, \ldots,\ p = -q, -q+2, \ldots, q,$$

where Z_m^k is the radial Zernike polynomial of degree m and order k, and in detector space the functions $\psi_{(p,q)}(s, \phi) = U_q(s)e^{ip\varphi}$, where $U_q(\cos(\kappa)) = \sin\left((q+1)\kappa\right) / \sin(\kappa)$ is the Chebyshef polynomial of the second kind. Moreover, the singular values of K_R are $\lambda_{(p,q)} = (q+1)^{-1/2}$, so that for $(p, q) \in \{0 \le q; p = -q, -q+2, \ldots, q\}$, $K_R\phi_{(p,q)} = \lambda_{(p,q)}\psi_{(p,q)}$.
The observational model is (1), where the design points $z_k \in [0, 1] \times [0, 2\pi)$ are an (at least approximately) orthogonal design for the basis functions $\psi_{(p,q)}$. The hypotheses (2) now describes the signal θ as a combination of finitely many functions $\phi_{(p,q)}$, where the value of q restricts the radial complexity of the signal, whereas p bounds its absolute angular frequency from above. In a two-sample problem, by taking differences one can also apply the methodology for testing equality of two images observed indirectly under the Radon transform.

3 Model testing

We consider testing the hypothesis that a function has a prescribed parametric form while not specifying a parametric alternative model. Such tests fall within the area of omnibus nonparametric methods. For an extensive overview of such methods, we refer to Hart (1997). In this paper we focus attention to two types of tests, namely the order selection test and the data-driven Neyman smooth type test.

3.1 The order selection test

Eubank and Hart (1992) proposed the use of order selection tests for testing the fit of a linear model in a fixed design regression model. The method starts with expressing the difference between the hypothesized linear function and the true regression function as an orthogonal series. For our hypothesis H_0' this corresponds to writing $(K\theta)_{H_0'} - (K\theta)_{\text{true}} = \sum_{j=1}^{\infty} b_{p+j}\psi_{p+j}$. A modified Mallows' (1973) criterion was used by Eubank and Hart (1992) to choose the number of terms in the series estimator. Their test can also be formulated as follows. Let

$$T_n' = \max_{1 \le m \le n-p} \frac{1}{m} \sum_{j=1}^{m} \frac{n\hat{b}_{j+p,n}^2}{\hat{\sigma}^2},$$

where $\hat{\sigma}^2$ is a consistent estimate of σ^2, cf. e.g. Munk et al. (2005). Eubank and Hart (1992) show that if $E\epsilon_1^4 < \infty$ and

$$\frac{1}{n}\sum_{k=1}^{n} \psi_i^2(z_k)\,\psi_j^2(z_k) \le C \tag{6}$$

for some $C > 0$ and all $p+1 \le i, j \le n$, under H_0' we have that

$$T_n' \xrightarrow{\mathcal{L}} T' := \sup_{m\ge 1} \frac{1}{m}\sum_{j=1}^{m} Z_j^2, \quad n \to \infty, \tag{7}$$

where $Z_1, Z_2, \ldots$ are i.i.d. standard normal random variables, and $\xrightarrow{\mathcal{L}}$ denotes convergence in distribution. According to (7), the hypothesis H_0' is rejected with asymptotic level $\alpha > 0$ if the value of T_n' exceeds the $(1-\alpha)$ quantile $q_{1-\alpha}$ of T'. For the quantile $q_{1-\alpha}$, explicit formulas are available; alternatively it can be determined by simulation. We shall call the test based on T_n' the classical order selection test, for further details concerning it cf. Eubank and Hart (1992) or Hart (1997). Note that the test statistic T_n' is based on the magnitude of estimates $\hat{b}_{j,n}$ of the Fourier coefficients $b_j =< K\theta, \psi_j >_{L^2(\mu_2)}$, $j = p+1, \ldots, n$, and thus measures the distance of $K\theta$ from the functions specified in H_0'. However, if one wants to detect deviations from the functions specified in the hypothesis H_0, a test which is directly based on the distance between θ and the function in H_0 seems to be more appropriate. Therefore, we suggest a test statistic which is based on the magnitude of estimates $\hat{a}_{j,n}^2$ of the Fourier coefficients $< \theta, \phi_j >_{L^2(\mu_1)}$. More precisely, consider

$$T_n \;=\; \max_{1\le m\le n-p} \frac{1}{\Lambda_m}\sum_{j=1}^{m} \frac{n\,\hat{a}_{j+p,n}^2}{\hat{\sigma}^2} \;=\; \max_{1\le m\le n-p} \frac{1}{\Lambda_m}\sum_{j=1}^{m} \frac{n\,\hat{b}_{j+p,n}^2}{\hat{\sigma}^2\lambda_{j+p}^2},$$

where $\Lambda_{m,p} = \Lambda_m = \sum_{j=p+1}^{p+m} 1/\lambda_j^2$, and

$$T = \sup_{m\ge 1} \frac{1}{\Lambda_m}\sum_{j=1}^{m} \frac{Z_j^2}{\lambda_{j+p}^2}. \tag{8}$$

The distribution of the supremum of the i.i.d. random walk, T', is explicitly available (cf. Spitzer, 1956), but the derivation depends heavily on symmetry arguments for the vectors $(Z_1^2 - 1, \ldots, Z_n^2 - 1)$. These arguments do not carry over to the case of T which is a supremum of *weighted* random walks. However, the following lemma shows that the distribution of T can be approximated arbitrarily well by simulations.

Lemma 1. *Suppose that the singular values satisfy (3). Then for $x > 1$ and $n \in \mathbb{N}$,*

$$P\Big(\sup_{m\ge n} \frac{1}{\Lambda_m}\sum_{j=1}^{m} \frac{Z_j^2}{\lambda_{j+p}^2} \ge x\Big) = O\big(\frac{1}{(x-1)^2 n}\big). \tag{9}$$

Furthermore, $P(1 \le T < \infty) = 1$.

In Figure 1 we have displayed the densities of truncated versions of T' and T for different decay of the eigenvalues, where we only consider $\sup_{1\le m\le 50}$ in (7) and (8). We truncate in order to achieve a better approximation of the distributions of T_{50} and T_{50}' in the subsequent

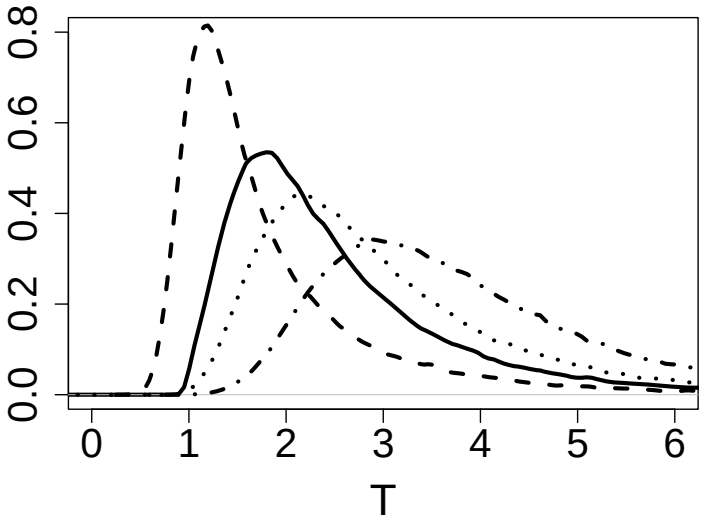

Figure 1: Simulated densities of T' (dashed line) and T for centered normal noise ($\sigma = 0.1$), where we use $\sup_{1\leq m\leq 50}$ in (7) and (8). The eigenvalues of T are $\lambda_i = i^{-1}$(solid), $\lambda_i = i^{-2}$(dotted), $\lambda_i = i^{-5}$(dashed-dotted), respectively. Note that due to truncation the simulated probabilites $P(T < 1)$ and $P(T' < 1)$ are non-zero, in contrast to the asymptotic limit.

simulations. Note that this truncation results in a small proportion of values for T and T' which are < 1. It is apparent from Figure 1 that the densities of T are more shifted to the right as the decay of the eigenvalues increases. This implies that using the non-adjusted distribution of T' instead of T for our tests would result in too liberal procedures.
The next theorem shows that asymptotic critical values for T_n are given by the critical values of T.

Theorem 2. *Suppose that in model (1), Assumption 1 is satisfied. Further suppose that the singular values of K satisfy (3) and that the singular functions (ψ_j) satisfy (6). Then under the hypothesis H_0 we have that for $x > 1$,*

$$P(T_n \leq x) \to P(T \leq x), \quad n \to \infty. \tag{10}$$

Let c_α denote the critical value at level α for the statistic T. Then the test which rejects when $T_n > c_\alpha$ is equivalent to the test which rejects when $\widetilde{j}_n > 0$, where

$$\widetilde{j}_n = \arg\max_{1\leq m\leq n-p} A_n(m) \quad \text{and} \quad A_n(m) = \sum_{j=1}^{m} \frac{n\hat{b}^2_{j+p,n}}{\hat{\sigma}^2\lambda^2_{j+p}} - c_\alpha\Lambda_m.$$

Therefore, if the null hypothesis is rejected, the value of $\widetilde{j}_n$ automatically suggests an alternative model which includes further basis functions. Similarly to the proof of Theorem 2, it

can be shown that $\widetilde{j}_n$ converges in distribution to

$$\widetilde{j} = \arg\max_{m\geq 1}\Big(\sum_{j=1}^{m} \frac{Z_j^2}{\lambda_{j+p}^2} - c_\alpha \Lambda_m\Big).$$

In order to get an impression of the theoretical power properties of tests based on T_n, we prove consistency of such a test under a fixed alternative. The argument follows along similar lines as in Hart (1997, p. 196) for the classical order selection test.

Theorem 3. *Suppose that there exist $\delta > 0$ and $j \geq 1$ such that*

$$\lim_{n\to\infty} P\big(\hat{b}_{j+p,n}^2 \geq \delta\big) \to 1. \tag{11}$$

Then $P(T_n \geq c_\alpha) \to 1$, as $n \to \infty$, for any $\alpha > 0$.

A further investigation of power properties of T_n in finite sample situations, in particular as compared to T_n', is provided in the simulation study in Section 4.

3.2 A data-driven Neyman smooth test

In a series of papers, Ledwina (1994) and Kallenberg and Ledwina (1995) introduced data-driven versions of Neyman's goodness-of-fit test for testing the fit of a density function. Such tests can also be transferred to the lack-of-fit problem in regression models, cf. Hart (1997) and Inglot and Ledwina (2006). The idea behind the data-driven Neyman smooth test is similar to the order selection test, though it has several important differences. First, the order is determined by the Bayesian information criterion BIC (Schwarz, 1978) where the maximized likelihood ratio value is replaced by the score statistic as follows. Define the sequence

$$S_n'(k) = \sum_{j=1}^{k} \frac{n\hat{b}_{j+p,n}^2}{\hat{\sigma}^2}, \quad k = 1, \ldots, n-p.$$

Then

$$\begin{aligned} B_n'(k) &= S_n'(k) - k\,\log n, \quad k = 1, \ldots, n-p, \\ \tilde{k}' &= \operatorname{argmax}_{1\leq k\leq n-p} B_n'(k). \end{aligned}$$

Second, the test statistic used is $S_n'(\tilde{k}')$, which is the score test at the chosen model order. A third difference is that in order to apply this test, the choice $k = 0$ is not allowed. Indeed, if it were allowed to obtain that $k = 0$, by consistency of the BIC as a model selection criterion, under the null hypothesis H_0' it would consistently select $\tilde{k}' = 0$, and hence not be usable as a test (see Ledwina, 1994). Then if $E\epsilon_1^4 < \infty$ and if (6) holds, one has that $P(\tilde{k}' = 1) \to 1$, and therefore

$$S_n'(\tilde{k}') \xrightarrow{\mathcal{L}} \chi_1^2.$$

The hypothesis is thus rejected with asymptotic level α if $S_n'(\tilde{k}')$ exceeds the $1-\alpha$ quantile of a chi-squared random variable with one degree of freedom. We shall call the test based on $S_n'(\tilde{k}')$ the classical data-driven Neyman smooth test.

For the hypothesis H_0, we propose a modified version of the data-driven Neyman smooth test which is based on estimates $\hat{a}^2_{j,n}$ of the Fourier coefficients $< \theta, \phi_j >_{L^2(\mu_1)}$. To this end define

$$S_n(k) = \sum_{j=1}^{k} \frac{n\hat{b}^2_{j+p,n}}{\hat{\sigma}^2 \lambda^2_{j+p}}, \quad k = 1, \ldots, n-p,$$

and consider the selection criterion $B_n(k) = S_n(k) - \Lambda_k \log n$, $1 \leq k \leq n-p$, $\tilde{k} = \text{argmax}_{1 \leq k \leq n-p} B_n(k)$.

Theorem 4. *Suppose that in model (1), the eigenvalues satisfy (3) and that the eigenfunctions satisfy (6). Then under the hypothesis H_0 we have that as n tends to infinity, $P(\tilde{k} = 1) \to 1$, and consequently that*

$$S_n(\tilde{k}) \xrightarrow{\mathcal{L}} Z^2/\lambda^2_{p+1},$$

where Z is standard normal.

The critical value of the data driven Neyman smooth test for inverse regression is determined by a chi-squared critical value with one degree of freedom, and by the eigenvalue λ_{p+1}, which corresponds to the first additional eigenvector used under the alternative hypothesis. This behavior is expected for a test for which the order is determined by the BIC, with penalty factor the log of the sample size. A consistency result against fixed alternatives, similar to Theorem 3, could also be proved for the inverse data-driven Neyman smooth test, by following the argument in Kallenberg and Ledwina (1995), which we, however, omit for brevity. The fact that the power of the data driven Neyman smooth test for local alternatives depends on the first coefficient in the alternative model was discussed in a study of goodness-of-fit tests in Claeskens and Hjort (2004); a similar conclusion about contiguous alternatives was reached by Inglot and Ledwina (2001).

Extensions to general spectral schemes. As pointed out by the associate editor both test statistics are special cases of

$$T_{f,n} \quad = \quad \max_{1 \leq m \leq n-p} \frac{1}{\sum_{j=p+1}^{p+m} 1/f(\lambda_j)^2} \sum_{j=1}^{m} \frac{n\,\hat{b}^2_{j+p,n}}{\hat{\sigma}^2 f(\lambda^2_{j+p})}.$$

Here $f \equiv 1$ for T_n' and $f(x) = x$ for T_n. More generally, one might consider a sequence of functions f_m possibly depending on m, s.t. $f_m \to f$. If one wants to obtain a consistent test based on θ (which is the goal of the present paper) and not on $K\theta$, then we stress that at least asymptotically $f_m(x) \to x$. Note, that in the spectral domain this corresponds to an approximation of the identity. Any choice other than a regularized version of $f(x) = x$ would yield a test which puts deviant weights on alternatives characterized by different Fourier coefficients $a_i \neq 0$. Nevertheless, this could be useful for the construction of tests with increased sensitivity against specific types of alternatives, however, its omnibus character would be violated. Interestingly, the choice of f_m is similar to the choice of a spectral regularization method (cf. Mair and Ruymgaart 1996). Indeed, there one uses a function $g(\lambda_j; \alpha)$ (which corresponds to f_m^{-2} and α corresponds to m^{-1}), depending on a regularization parameter $\alpha > 0$. In particular, one requires $g(\lambda_j; \alpha) \to \lambda_j^{-2}$ for $\alpha \to 0$. The version we use corresponds to spectral cut-off estimation (cf. Mair and Ruymgaart 1996, p. 1426). Note that due to the form of the test statistic T_n as a maximum, a choice of the truncation parameter m is not required, which is quite an advantage of the method. One might also wish to regularize additionally

the function f, similar to tapering in orthogonal series estimation. Then one would require an additional parameter, say $N(n) \to \infty$, and one could use e.g. $\lambda_j^2/(N(n)^{-1} + \lambda_j^2)^2$ instead of λ_j^{-2}. For estimation, it is well known that this can reduce the finite sample MSE. For testing, such an additional regularization step does not seem to be necessary as the level of our method is kept quite accurately (cf. Section 5).

The case of estimated K. We close this section with a brief discussion for testing in model (1) if there is additional noise in the operator K. Concerning estimation purposes there has been some recent work in this direction (cf. Hoffmann and Reiß, 2007; and Cavalier and Hengartner, 2005). Generally speaking, if the whole operator K has to be estimated (cf. Hoffmann and Reiß, 2007), our indirect approach would involve estimation of the functions ϕ_j, ψ_j and the singular values λ_j, which is infeasible. Further, hypotheses of type (4) cannot be interpreted if the functions ϕ_j are unknown.

In contrast, if only the eigenvalues are unknown but can be estimated (Cavalier and Hengartner, 2005), our approach will be useful in general. In a white noise model, Cavalier and Hengartner (2005) show that as long as the noise level in the eigenvalues is less or equal to the noise level in the function $K\theta$, the rate is the same as for known eigenvalues. In our context of hypothesis testing, we expect that the asymptotic distribution of the test statistics remains the same if the noise level in the eigenvalues is less than the noise level in $K\theta$. A full analysis of this issue is beyond the scope of this paper, however, a small simulation study in the next section confirms the above statement.

4 Simulation study

In this section we describe the results of a simulation study of the (inverse) order selection and the (inverse) Neyman smooth tests based on the statistics T_n and S_n, respectively, and compare it to their classical (direct) counterparts, based on statistics T_n' and S_n'. For this purpose, we generate data from model (1), where K is a convolution operator on $[0,1]$. The kernel of the convolution integral is defined by choosing its eigenvalues for the system of eigenfunctions $\phi_j(x) = \sqrt{2}\cos(2\pi jx)$ to decay as $\lambda_j \sim 1/j$.

First we discuss the order selection test. In Fig. 2 we compare the empirical distribution functions, based on 1000 simulations, of the test statistic T_n for $n = 50, 500$, respectively, with the distribution function of the asymptotic statistic T. The noise terms ε_k have standard deviation 0.1 and are distributed either normally or according to a t-distribution with 10 degrees of freedom. Note from the figure that the empirical distribution of T_n approximates already closely its asymptotic shape, given by the distribution of T, for rather small sample sizes. For the $t-$distributed noise, which is the more difficult case, the distribution of T_{500} is hardly distinguishable from the distribution of T, and for the normal case this is even more true.

In the second part of the simulations we generated data from certain alternatives, where we assume that one of the Fourier coefficients a_j of θ is now nonzero, and the noise is normally distributed. Moreover, we both consider the case $p = 0$ (or, in more detail, $H_0 : a_j = 0$ for all j, i.e. hypothesis (2) with $p = 0$, which effectively tests the signal for being zero), and the non-trivial null hypothesis $p = 3$, where we generate artificial data with $\theta_{3:1} : (a_1, a_2, a_3) = (1/10, 1/10, 1/10)$ and $\theta_{3:2} : (a_1, a_2, a_3) = (1/10, 1/20, 1/30)$. For every combination of parameters we have repeated 20 times the following procedure and averaged the resulting powers. First, the critical values for the test were estimated from 500

Table 1: Simulated power (%) of the classical and inverse order selection and Neyman smooth tests for levels $0.2, 0.1$ and 0.05 from 500 simulation runs. The sample size is either 100 or 500, and σ equals either 0.1 or 0.01. Several choices for the coefficients a_1, a_5 and a_{10} are considered, and "hypoth." indicates that the simulations of the power have been performed under the null hypothesis, generating data from the function given in the first column.

				Order selection test						Neyman smooth test					
				Power classical test			Power inverse test			Power classical test			Power inverse test		
				Level			Level			Level			Level		
H_0	n	σ	Altern.	0.2	0.1	0.05	0.2	0.1	0.05	0.2	0.1	0.05	0.2	0.1	0.05
$p = 0$	100	0.1	$a_1 = 0.01$	36	24	15	32	19	12	39	24	11	38	21	7
			$a_5 = 0.03$	21	11	6	23	12	6	20	10	5	21	10	6
			$a_5 = 0.1$	36	18	8	46	29	18	23	14	9	33	26	21
			$a_5 = 0.3$	100	99	97	100	100	100	98	98	98	100	100	100
			$a_{10} = 0.3$	35	14	6	56	34	19	20	11	5	36	28	24
			$a_{10} = 1$	100	100	100	100	100	100	100	100	100	100	100	100
	500	0.1	$a_5 = 0.1$	94	82	63	98	95	90	54	48	45	86	85	84
			$a_{10} = 0.1$	27	12	6	35	18	8	19	10	5	20	11	6
			$a_{10} = 0.3$	100	97	83	100	100	100	53	48	45	99	98	98
	100	0.01	$a_1 = 0.003$	93	89	83	89	84	77	95	89	76	95	86	47
			$a_5 = 0.01$	36	18	8	46	30	19	22	13	8	34	26	22
$p = 1$	100	0.1	$a_5 = 0.1$	41	21	10	48	30	18	27	19	14	36	29	25
			$a_{10} = 0.3$	25	10	3	36	24	13	20	11	6	37	29	25
			hypoth.	21	10	5	19	10	5	21	10	5	20	10	5
$p = 3$, $\theta = \theta_{3:1}$	100	0.1	$a_5 = 0.1$	57	41	28	57	42	29	54	48	42	54	48	44
			$a_{10} = 0.3$	52	22	8	66	46	26	26	15	11	42	33	30
			hypoth.	20	11	6	19	11	5	20	10	5	20	10	5
$p = 3$, $\theta = \theta_{3:2}$	100	0.1	$a_5 = 0.1$	58	42	29	57	43	31	54	48	42	54	48	44
			$a_{10} = 0.3$	50	25	9	63	44	27	24	15	10	40	32	28
			hypoth.	21	10	5	19	10	5	19	10	5	19	10	5
$p = 0$, σ est.	100	0.1	$a_5 = 0.1$	36	17	8	47	32	19	23	14	10	34	26	22
			$a_{10} = 0.3$	38	17	7	56	36	21	22	12	6	37	29	25
	100	0.1	hypoth.	21	10	6	21	13	7	22	11	7	22	12	7
$p = 3$, $\theta = \theta_{3:1}, \sigma$ est.			$a_{10} = 0.3$	51	26	12	65	47	31	24	15	10	38	31	28
			hypoth.	23	11	6	24	13	6	21	11	7	21	11	6
$p = 0$, $\hat{\lambda}_j$ add. err.	100	0.1	hypoth.	19	11	6	20	11	6	20	10	5	20	9	5
			$a_5 = 0.1$	35	19	8	36	22	13	24	15	8	34	23	8
$p = 0$, $\hat{\lambda}_j$ mult. err.	100	0.1	hypoth.	21	10	5	20	9	5	20	10	4	20	9	4
			$a_5 = 0.1$	35	17	8	45	28	17	23	13	8	33	23	19

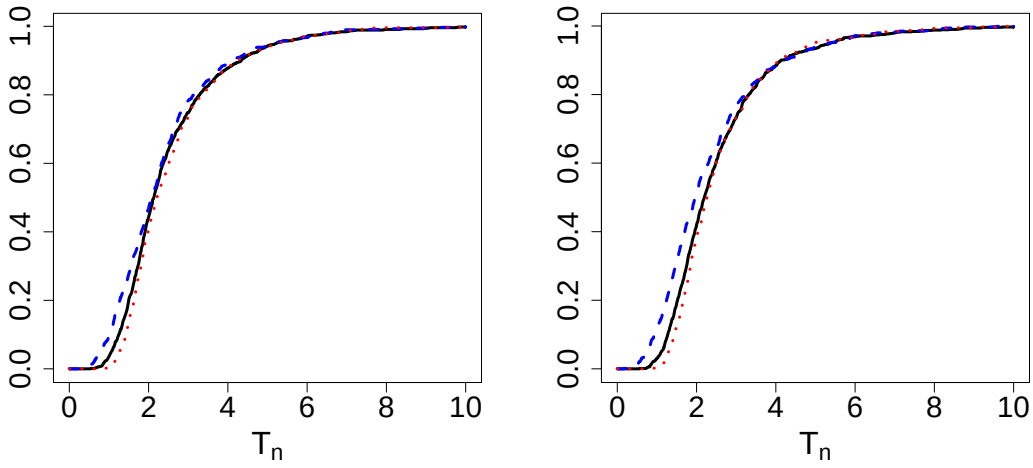

Figure 2: Simulated distribution functions of T_{50} (dashed line), T_{500} (dotted line) and T (solid line) for simulations with normal noise (l.h.s.) and for simulations with t-distributed noise with 10 degrees of freedom (r.h.s.).

simulations, and in the second step used to determine the power of the test in another 100 simulations. Hence, we have computed 2000 simulations for each combination of parameters to determine the power of the test, grouped into blocks of 100 simulations for which we re-simulated the critical value of the test to include both the randomness in the simulated critical values and in the observed data. Finally, we also considered the case that the eigenvalues λ_j are unknown, but estimates from additional observations are available. First, we performed simulations where we assume that the estimated eigenvalues $\hat{\lambda}_j$ are disturbed by an additive error, with error terms distributed i.i.d. normal with standard deviation 0.05 and mean 0. Second, we considered multiplicative noise, distributed according to a truncated normal distribution with standard deviation 0.05 (but now mean 1), where the truncation was performed symmetric to the mean and such that negative values of the noise factor were avoided. In both scenarios we used critical values for the tests based on simulations with the estimated (noisy) eigenvalues, and generated the observations used in the subsequent tests based on the true (in practice unknown) eigenvalues as given above.

In Table 1 (left-hand side) we compare the power of the inverse order selection test with its classical counterpart (where the latter is based on the statistic T_n') for a number of combinations of the design sample size n, the noise standard deviation σ, and the index j and value a_j of a non-zero Fourier coefficient of θ. The critical values for the tests for levels of $0.05, 0.1$ and 0.2 were determined from the simulations under $H_0 : a_j = 0$ for all j. In a similar way, we performed simulations of the inverse and classical Neyman smooth tests for the same settings as for the order selection test. The critical values used were again determined from simulations under $H_0 : a_j = 0$ for all j. The right-hand side of Table 1 gives the results for the simulated power of the inverse and classical (direct) Neyman smooth test.

We draw the following conclusions from Table 1. For the case of low frequency alternatives (notably the case $p = 0$, $a_1 \neq 0$), the classical (direct) tests perform somewhat better than the

inverse tests. Here, the increase of the critical values due to assigning larger weights to high frequency components results in a slight loss of power for the inverse tests. In most of the other scenarios, the inverse tests outperform their classical (direct) counterparts. Moreover, the inverse order selection is superior to the inverse Neyman test in the majority of cases, with again an exception for the lowest frequency alternative. In more detail, for both types of tests and $H_0 : p = 0$, the power decreases at fixed level of the perturbation with the order of the affected eigenfunction due to the decrease of the corresponding eigenvalue. An increase in the sample size or a reduction in the variance of the noise yields significant increases in the power (at fixed type and level of the perturbation). The power against perturbations in the 5^{th} or 10^{th} eigenfunction increases if the null is changed to $H_0 : p = 3$. This is due to the fact, that the associated eigenvalues are now 4/5 and 4/10 of the largest eigenvalue λ_4 in the alternative, instead of 1/5 and 1/10 compared to λ_1 under $H_0 : p = 0$. However, the choice of the true function $\theta = \theta_{3:1}$ or $\theta = \theta_{3:2}$ is not important. Note that the simulations with non-trivial null hypothesis and testing data generated under the null show that the test approximately keeps its level; this holds both for the simulations with simple null hypothesis $H_0 : p = 0$ and the non-trivial case $H_0 : p = 3$. Next, estimation of the variance with a simple difference estimator (Rice, 1984) results in a slight exceedance of the nominal level which in turn leads to an apparent increase in the power of the order selection test at given perturbation type and level for $H_0 : p = 3$, as compared to the case for known variance σ^2. Finally, if the eigenvalues have to be estimated, the tests still perform reasonably well.

5 Application to confocal fluorescence microscopy

5.1 Modelling the observations

Fluorescence microscopy at nanoscales is often hampered by poor signal-to-noise ratios of the individual image frames. Hence, in general a series of several image frames is taken consecutively and accumulated or averaged to yield a single image. However, this has the disadvantage that slight movement of the object table or of the observed object, e.g. in live cell imaging, results in an additional blur of the final image. This could be avoided by testing the individual image frames for significant differences, and, possibly, proper image registration before accumulation of the individual frames. Another relevant application is automatic tracking of structural changes within the imaged object over a long time period. For example, GFP (green fluorescent protein)-tagged proteins are used to detect structural changes of intracellular organelles caused by mutations in this protein and for pharmacological tests (cf. Pepperkok and Ellenberg, 2006, for automatic microscopy). Similarly, the monitoring of the motion of intracellular objects such as proteins or transport compartments is of substantial interest. To this end, it is important to note that the image map which describes the microscope is strongly localized, i.e. there is a close correspondence between loci on the observed image and those in the true object. Hence, if we aim to detect changes at certain regions of the cell, it is tempting to restrict the analysis to a suitable part of the image.
In this section we will demonstrate the ability of our inverse testing procedure to detect significant image differences, which can e.g. be used to decide whether single frames may be accumulated straightforwardly. We will first introduce the specific hypotheses to be tested in this application, then introduce the deconvolution model for the data, and finally present the results from an application to a (typical) sequence of images of fluorescently labeled living cells acquired with a confocal laser scanning microscope (Leica TCS).

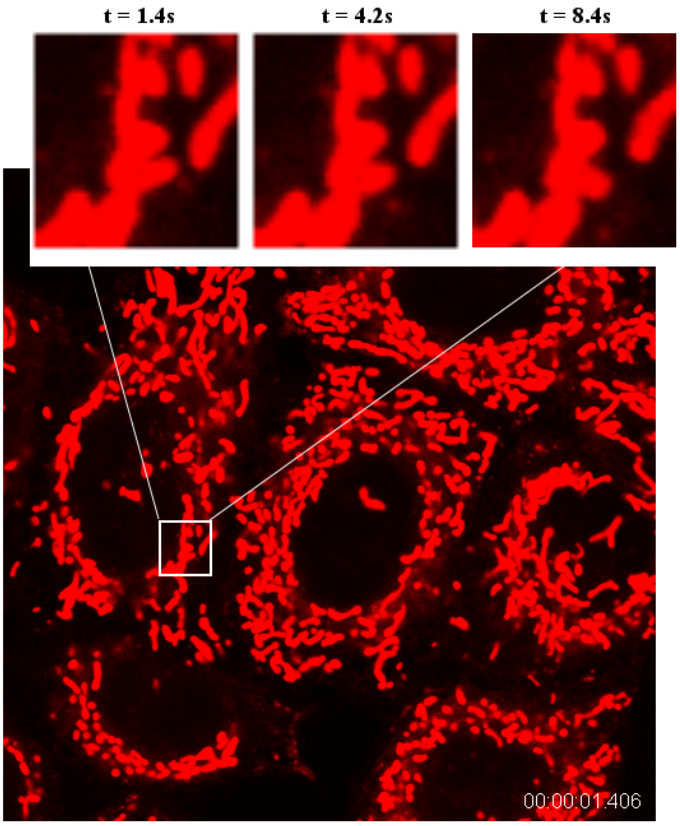

Figure 3: Light microscopic image of fluorescently labeled intracellular membrane structures in HeLa cells (cervix cancer cell line) using the lipophilic carbocyanine dye DiI (red). In the small sub-images we focus on a typical example for alterations in the imaged object due to biological processes in the cells. It shows the movement of a tubular membrane compartment, which may serve as transport or carrier for proteins. Detection of such compartments helps to illucidate intracellular trafficing pathways.

Our aim is to assess the significance of differences between two images of the same object. Hence, we apply our test to the following null hypothesis:

$$H_0 : \ I_1 = cI_2$$

where I_1 and I_2 represent the intensity distributions of the first and second image, respectively, and $c > 0$ is a (real) constant which allows for different exposure times of the images. The constant c can be estimated straightforwardly from the data by taking the ratio of the means of the two images. Since the estimate $\hat{c}$ always was very close to one (with standard deviation approx. 1%) we have not considered the additional estimation error any further.
Next we introduce the model for such data obtained from confocal microscopy. Typically, available are count data representing observed image intensities on a two- or three-dimensional, equidistant, grid of design-points in the unit square or cube. Here, we consider the two-dimensional case, however the extension to three-dimensional data is straightforward. The

design points are given by

$$z_{jk} = \left(\frac{2j-1}{2n}, \frac{2k-1}{2n} \right), \, 1 \leq j,k \leq n.$$

Hence, at our disposal are observations $Y_{jk} = (K\theta)(z_{jk}) + \varepsilon_{jk}$, where

$$(K\theta)(z) = g * \theta(z) = \int_{[0,1]^2} g(z-t)\theta(t)\, dt,$$

where "$*$" represents the convolution of the periodic functions $\theta, g \in L^2([0,1]^2)$, and g is called the point-spread-function [PSF] of the microscope. The PSF describes the imaging process and may be computed from the optical properties of the microscope. It represents the image of a point-source observed by the respective microscope. The convolution with the PSF amounts to a smoothing of the original image of the object, where typical smoothing scales are of order $\approx 100nm$. However, often the biological structures of interest within the imaged object are of comparable size, and it therefore is necessary to compensate for the convolution of the image with the PSF. Finally, the standard model for the distribution of the photon count data Y_{jk} is $Y_{jk} \sim \text{Poiss}\,[(K\theta)(z_{jk})]$, all independent. Hence, the distribution of each pixel $\tilde{Y}_{jk}$ of the difference image $I_1 - \hat{c}I_2$ is given by the difference of two (scaled) Poisson variables. This model implies that the noise of the observations $\tilde{Y}_{jk}$ is not homoscedastic. However, as will be discussed in more detail in Section 5.2, the large number of design points $(10000 - 25000)$ in our application counterbalances this potential problem sufficiently.
We now discuss briefly the properties of the operator K which is needed to apply the inverse tests. Note that the linearity of the operator K implies that $E\tilde{Y}_{jk} = K(\theta_1 - c\theta_2)$, where $\theta_1 - c\theta_2$ is the difference of the (unknown) true intensity distributions of the first and second image I_1 and I_2. The spectral transform for the convolution operator is given by the Fourier transform on $[0,1] \times [0,1]$. Hence, the eigenfunctions of K are $\phi_{j,k}(t) = \exp(2\pi i((j,k) \cdot t)$, $(j,k \in \mathbb{Z})$ and $t \in \mathbb{R}^2$, and its eigenvalues are

$$\lambda_{j,k} = \int_{[0,1]^2} g(t)\, e^{-2\pi i((j,k)\cdot t)}\, dt, \qquad j,k \in \mathbb{Z}.$$

The Fourier coefficients $b_{j,k,n}$ of $K\theta$ can then be estimated by

$$\hat{b}_{j,k,n} = \frac{1}{n^2} \sum_{l=1}^{n} \sum_{\tilde{l}=1}^{n} \tilde{Y}_{l,\tilde{l}} \phi^*_{j,k}(z_{l,\tilde{l}}),$$

and those of the original image θ by $\hat{a}_{j,k,n} = \frac{\hat{b}_{j,k,n}}{\lambda_{j,k}}$.
Now we comment on the implementation of the order selection test for the specific setting under consideration here. A similar reasoning holds true for the Neyman smooth test. In contrast to the one–dimensional case considered in Section 3.1 there does not exist a natural ordering of the eigenvalues by the index of the eigenfunctions anymore. We use the following test statistics for the test of the hypothesis H_0 of zero difference between signals, as defined above. It is based on a surrogate to the one–dimensional ordering of the eigenvalues based on the Euclidean norm of their index pairs (j,k):

$$T_n = \max_{1 \leq r_l \leq \sqrt{2n^2}} \frac{1}{\Lambda_{r_l}} \sum_{1 \leq j^2+k^2 \leq r_l^2} \frac{n^2 |\hat{a}_{j,k,n}|^2}{\hat{\sigma}^2},$$

Time stamps 1st/ 2nd frame in sec.	1.4	2.8	4.2	5.6	7.0	8.4	9.8	11.25
1.4	-	90/89	3	6/18	0	0	0	0
2.8	90/89	-	1	18/40	0	0	0	0
4.2	3	1	-	3/14	1	0	0	0
5.6	6/18	18/40	3/14	-	2	0	0	0
7.0	0	0	1	2	-	32/41	5/4	5/13
8.4	0	0	0	0	32/41	-	68/55	20/43
9.8	0	0	0	0	5/4	68/55	-	31/22
11.25	0	0	0	0	5/13	20/43	31/22	-

Table 2: P-values of the inverse order selection test (left) and the inverse data-driven Neyman smooth test (right) for testing the null hypothesis that two specific images in the time sequence are identical up to a scaling constant and noise (for a single number the P-values of the two tests are equal).

where r_l is the ordered sequence of values of $\sqrt{j^2+k^2}$ for $-n \leq j,k \leq n$ (with $j,k \in \mathbb{Z}$), and $\hat{\sigma}^2$ is an estimator of $\sigma^2 = E\varepsilon^2$. In our computations we used the following bivariate difference scheme estimator (Munk et al., 2005)

$$\hat{\sigma}^2 = \frac{1}{2n(n-1)} \sum_{1\leq l\leq n, 1\leq \tilde{l}\leq n-1} \left(\tilde{Y}_{l,\tilde{l}+1} - \tilde{Y}_{l,\tilde{l}}\right)^2.$$

The data considered here are real-valued, hence it follows that $a_{j,k,n} = \overline{a}_{-j,-k,n}$, and we compare the realized value t_n of T_n computed from the data with the quantiles of the simulated distribution of

$$T = \sup_{1\leq r_l} \frac{1}{\Lambda_{r_l}} \sum_{1\leq j^2+k^2\leq r_l} \frac{Z_{j,k}^2}{|\lambda_{j,k}|^2},$$

where $Z_{j,k} := Z_{-j,-k} \sim N(0,1)$, and $\Lambda_{r_l} = \sum_{1\leq j^2+k^2\leq r_l} \frac{1}{|\lambda_{j,k}|^2}$.

5.2 Application to the HeLa data

We use our method now to compare single image frames in a sequence of confocal images of living HeLa cells, an established cell line. The standard imaging procedure in this case would be to accumulate a certain number, say 4, images of the same object at the same position to improve the signal-to-noise ratio. In our case, there are 9 images which have been acquired in a total time period of ≈ 11.25 seconds. Their voxel size is $138.9nm$ in x and y-direction, which corresponds to a zoom level of 2.5. To speed up computations, we focus on a sub-image with size of 101×101 pixels close to the middle of fig. 3 which contains both cell membrane and cell interior, in order to be representative of the structure of the image.
Table 2 gives the result of the application of the inverse order selection and the inverse Neyman smooth tests to a number of comparisons of image pairs from this sequence (the results for the direct tests were similar). From the results we find that, for images acquired within $\approx 2-3$s, the null is in many cases not rejected to within a level of 5%, whereas the images are significantly different for image pairs taken at larger time intervals. This implies

that care has to be taken before images taken at larger intervals are accumulated. A detailed visual inspection of the image sequence indeed confirms that the images both change w.r.t. large scale movements, and w.r.t. to changes of small scale features such as moving vesicles, which is to be attributed to actual changes of the object (cf. fig. 3). Concluding, the analysis indicates that the test is sensitive enough to detect actually existing image changes, wheres it is not over-sensitive, in the sense that the null is not rejected for several image pairs, which are in most cases images captured in immediate sequence (e.g. those at timestamps 1.4s and 2.8s).

The HeLa data has been obtained with a standard confocal laser scanning microscope, where the PSF can be modeled well by a unimodal function. However, higher resolution images (particularly in the $z-$direction) can be obtained from more sophisticated fluorescence microscopes such as I^5M or $4PI$-microscopes, where a higher resolution is achieved by a more complicated PSF with strong sidelobes in the $z-$direction (cf. Bewersdorf et al., 2006). Therefore, it is here even more important than for confocal microscopy to include the deconvolution into the test statistics. Again, we suggest to use our testing procedure to detect changes in the image due to real changes in living cells, and to find image misalignements prior to image averaging. Related deconvolution settings where image changes and misalignment are important to detect exist in many fields. Here we mention laser ophthalmoscopy (e.g. Nourrit et al., 2005), where it is of interest to detect changes of the human retina (after correction for image changes due to eye movements).

We close this section with a discussion of some of the assumptions required in Theorems 2 and 4. For our theoretical results we assume the noise to be homoscedastic. In contrast to this, the image data is (approximately) Poisson distributed, and hence the homoscedasticity assumption does not hold. However, the empirical Fourier coefficients $\hat{b}_{j,k,n}$ are computed from the sum of a very large number of design points ($10000-250000$ depending on the image geometry), which counterbalances this potential problem sufficiently. Indeed, some additional numerical simulations show that the test is somewhat conservative in this setting, but still performs reasonably well, if the number of design points is sufficiently large. In more detail, we performed simulations under the null hypothesis as follows. Two artificial images with Poisson noise were generated, where the pointwise Poisson means are based on a smoothed version of the HeLa image at the (first) time step $1.4s$. The smoothing was performed by averaging any point with its four immediate neighbours. In one of these images, the Poisson means were rescaled with a scaling factor $\bar{c}$ which was selected randomly distributed according to a uniform distribution with mean one and standard deviation $\approx 2\%$, which is the typical variability between the total intensities of the HeLa images used here. In 100 simulations, the inverse order selection test rejected in 17, 13 and 2 simulations for levels 0.2, 0.1 and 0.05, respectively, and the inverse Neyman smooth test in 17, 9 and 3 cases. Finally, the PSF of a fluorescence microscope (e.g. of confocal or $4PI$ type) is band-limited, i.e. only has finitely many non-zero Fourier coefficients. This implies that it is not possible to attain any information on the object at scales smaller than approximately the Nyquist frequency. Hence, we actually only consider the Fourier transforms of the functions θ and $K\theta$ within the support of the OTF (i.e. the Fourier transform of the PSF), where assumption (3) on the OTF is not necessary anymore.

6 Discussion: Connections to model selection and extensions

Both order selection and data-driven Neyman smooth tests have a strong connection to model selection methods. We first define the AIC and BIC in their original framework, then we make a link back to the test statistics, and we proceed by proposing adjusted AIC and BIC versions which can be used in inverse regression problems.
The criteria AIC and BIC are originally derived in a likelihood setting. Let $\ell_n(\gamma)$ denote the log likelihood function of $Y_1, \ldots, Y_n$, with unknown parameter vector γ. In the direct normal linear regression setting, for example, where $Y_i = \beta_1\phi_1(x_i) + \ldots + \beta_p\phi_p(x_i) + \varepsilon_i$ and the independent errors $\varepsilon_i \sim N(0, \sigma^2)$, the log likelihood function is based on the normal density, and the parameter vector $\gamma_p = (\sigma^2, \beta_1, \ldots, \beta_p)$. For hypothesis testing, the null hypothesis

$$H_0 : E(Y|x) = \theta(x) = \sum_{j=1}^{p} \beta_j\phi_j(x)$$

is contrasted with the alternative hypothesis

$$H_a : \theta(x) = \sum_{j=1}^{k} \beta_j\phi_j(x) \text{ for some } k > p.$$

For each value of $k = p, p+1, \ldots$ there is a corresponding maximized log likelihood function $\ell_n(\hat{\gamma}_k)$. Hence, to each of the possible models under H_a, corresponds a value of the criteria

$$\mathrm{AIC}'(k) = 2\ell_n(\hat{\gamma}_k) - 2(k+1), \quad \mathrm{BIC}'(k) = 2\ell_n(\hat{\gamma}_k) - \log(n)(k+1),$$

where $k+1$ =length(γ_k). Maximizing these criteria is equivalent to maximizing the differences

$$\begin{aligned} \mathrm{aic}'(k) = \mathrm{AIC}'(k) - \mathrm{AIC}'(p) &= 2\{\ell_n(\hat{\gamma}_k) - \ell_n(\hat{\gamma}_p)\} - 2(k-p) \\ \mathrm{bic}'(k) = \mathrm{BIC}'(k) - \mathrm{BIC}'(p) &= 2\{\ell_n(\hat{\gamma}_k) - \ell_n(\hat{\gamma}_p)\} - \log(n)(k-p), \end{aligned}$$

for $k = p, p+1, \ldots$. We recognize the log likelihood ratio statistic. For normal data, up to a constant not depending on k, this statistic is equal to $n\{\log(\mathrm{SSE}_p) - \log(\mathrm{SSE}_k)\}$, where the error sum of squares $\mathrm{SSE}_k = \sum_{i=1}^{n}(Y_i - \hat{\beta}_1\phi_1(x_i) - \ldots - \hat{\beta}_k\phi_k(x_i))^2$. The likelihood ratio statistic is first order equivalent to the score statistic S_k. To define S_k, denote by r_n an upper bound for the values of $k-p$, and let $\tilde{\gamma}_k$ be the estimator of γ_k under the null hypothesis, that is, where $\beta_{p+r} = 0$ for $r = 1 \ldots, r_n$, hence the vector of length $p + r_n + 1$, $\tilde{\gamma}_k = (\hat{\gamma}_p, 0, \ldots, 0)$. Further, define $J(\gamma)$ the corresponding Fisher information matrix, with $J_{k,k}^{-1}$ its submatrix of dimension $(k-p) \times (k-p)$ in the lower right corner. Then,

$$S_k = \left(\frac{\partial\ell_n(\tilde{\gamma}_k)}{\partial\beta_{p+r}}\right)_{r=1,\ldots,k}^{t} J_{kk}^{-1}(\tilde{\gamma}_k) \left(\frac{\partial\ell_n(\tilde{\gamma}_k)}{\partial\beta_{p+r}}\right)_{r=1,\ldots,k}.$$

For the regression model as in (1) under the orthogonality assumption (and for now assuming normality) $S_k = S_n'(k)$ is the score statistic in the direct case if $\hat{\sigma}^2$ is the maximum likelihood estimator. For the data-driven Neyman smooth test the connection to the BIC is now immediate, using the score statistic instead of the log likelihood ratio statistic. For the order selection test, there is a resemblance to the AIC, with a fixed penalty of c_α times the value Λ_k. In the traditional AIC, $c_\alpha = 2$.

For indirect regression problems, the value Λ_k plays the role of the effective number of parameters in the model. This value is arrived at via arguments in the last part of the proof of Lemma 1. Hence, for inverse regression problems, the penalty is not the number of coefficients in the model, but rather the *weighted* number of coefficients, where the weights are the eigenvalues of the integral operator K.
Based on the reasoning above, we propose two new model selection criteria that are versions of the AIC and BIC type model selection methods for use in inverse regression problems. The criteria read as follows:

$$\mathrm{aic}(k) = \sum_{j=1}^{k} \frac{n\hat{b}_{j+p,n}^2}{\hat{\sigma}^2\lambda_{j+p}^2} - 2\Lambda_k, \quad \mathrm{bic}(k) = \sum_{j=1}^{k} \frac{n\hat{b}_{j+p,n}^2}{\hat{\sigma}^2\lambda_{j+p}^2} - \log(n)\Lambda_k. \tag{12}$$

The order k for which the criterion takes on the largest value is selected as the best model order for the given data. It is illustrative to consider polynomially decaying eigenvalues as in (3) which gives, e.g.

$$\mathrm{bic}(k) \propto \sum_{j=1}^{k} n(j+p)^{2\beta} \frac{\hat{b}_{j+p,n}^2}{\hat{\sigma}^2} - \log(n)\left(k^{2\beta+1} + O(k^{2\beta})\right). \tag{13}$$

Hence, instead of penalizing with the dimension of the model k a much stronger penalty $k^{2\beta+1}$ is required. To our knowledge only Loubes and Ludeña (2004) deal explicitly with model selection in the context of penalized estimation for (nonlinear) inverse problems. In particular, our criterion $\mathrm{aic}(k)$ in (12) is related to one of their selection criteria, cf. Remark 3.6 in Loubes and Ludeña (2004). In a related approach, Butucea and Comte (2007) investigate estimation based on model selection of a linear functional of θ in density deconvolution.

We conclude by mentioning some topics for future work. Even though testing for functions that are linear combinations of eigenfunctions covers a range of interesting applications, including testing for equality of two images, there are situations where other hypothesis tests are called for. In such situations, an orthogonalization approach can be included to make the basis functions that occur in the null hypothesis orthogonal to the eigenfunctions of the kernel, something which imposes both technical and practical complications.
The model selection question above translates to an order selection issue. Other interesting model selection problems arise with multivariate data. For example, when the variable z is multivariate, interest may lie in selecting components of z to be included in the model. It would be of great interest to see how this methods are capable to deal with sparseness assumptions.

Acknowledgements

We like to thank the editor, the associate editor and the referees for their constructive remarks and careful reading. Hajo Holzmann and Axel Munk would like to acknowledge financial support of the Deutsche Forschungsgemeinschaft, Grant MU 1230/8-2, Axel Munk support of the DFG/ SFB755 Nanoscale Photonic Imaging and DFG-FOR916, Nicolai Bissantz support of DFG /SFB475, and Axel Munk and Nicolai Bissantz of the BMBF Projekt INVERS. The work was initiated during a stay of Gerda Claeskens in Göttingen, which was financially supported by the DFG Graduiertenkolleg 1023 "Identifikation in Mathematischen Modellen".

The authors are especially grateful to Kathrin Bissantz (University of Münster, Germany) for providing the fluorescence microscopy images, and for help with the biological background.

References

Aerts, M., Claeskens, G. and Hart, J. D. (1999), Testing the fit of a parametric function. *J. Am. Statist. Assoc.* **94**, 869–879.

Aerts, M., Claeskens, G. and Hart, J. D. (2000), Testing lack of fit in multiple regression. *Biometrika* **87**, 405–424.

Akaike, H. (1973), Information theory and an extension of the maximum likelihood principle. *Second International Symposium on Information Theory*, B. Petrov and F. Csáki (editors), 267–281, Akadémiai Kiadó, Budapest.

Bewersdorf, J., Egner, A. and Hell, S. W. (2006), 4Pi Microscopy. In: Handbook of Biological Confocal Microscopy, ed. Pawley, J., 561–570, Springer, New York.

Bhattacharya, R. N. and Rango Rao, R. (1976), *Normal Approximation and Asymptotic Expansions*. Wiley, New York.

Billingsley, P. (1968), *Convergence of Probability Measures*, Wiley, New York.

Bissantz, N., Munk, A. and Scholz, A. (2003), Parametric versus non-parametric modeling? Statistical evidence based on P-value curves. *Mon. Not. R. Astron. Soc.* **340**, 1190–1198.

Bissantz, N., Hohage, T., Munk, A. and Ruymgaart, F. (2007), Convergence rates of general regularization methods for statistical inverse problems. *SIAM J. Num. Analys.* **45**, 2610–2636.

Butucea, C. and Comte, F. (2007), Adaptive estimation of linear functionals in the convolution model and applications. Preprint.

Cavalier, L. (2000), Efficient estimation of a density in a problem of tomography. *Ann. Statist.* **28**, 630–647.

Cavalier, L. and Tsybakov, A. (2002), Sharp adaptation for inverse problems with random noise, *Probab. Theory Relat. Fields* **123**, 323–354.

Cavalier, L. and Hengartner, N. W. (2005), Adaptive estimation for inverse problems with noisy operators. *Inverse Problems* **21**, 1345–1361.

Chow, Y. S. and Teicher, H. (1978), *Probability theory. Independence, interchangeability, martingales.* Springer-Verlag, New York-Heidelberg.

Claeskens, G. and Hjort, N. L. (2004), Goodness of fit via nonparametric likelihood ratios, *Scand. J. Statist.* **31**, 487–513.

Eubank, R. L. and Hart, J. D. (1992), Testing goodness-of-fit in regression via order selection criteria. *Ann. Statist.* **20**, 1412–1425.

Fan, J. (1991), On the optimal rates of convergence for nonparametric deconvolution problems. *Ann. Statist.* **19**, 1257–1272.

Goldenshluger, A. and Spokoiny, V. (2006) Recovering convex edges of an image from noisy tomographic data. *IEEE Trans. Inform. Theory* **52**, 1322–1334.

Hart, J. D. (1997), *Nonparametric smoothing and lack-of-fit tests.* Springer, New York.

Hoffmann, M. and Reiß, M. (2007), Nonlinear estimation for linear inverse problems with error in the operator. *Ann. Statist*, to appear.

Holzmann, H., Bissantz, N. and Munk, A. (2007), Density testing in a contaminated sample. *J. Multivar. Anal.* **98**, 57–75.

Inglot, T. and Ledwina, T. (2001), Intermediate approach to comparison of some goodness-of-fit tests. *Ann. Inst. Stat. Math.* **53**, 810–834.

Inglot, T. and Ledwina, T. (2006), Data-driven score tests for homoscedastic linear regression model: asymptotic results. *Probab. Math. Statist.* **26**, 41–61.

Johnstone, I. M., Kerkyacharian, G., Picard, D. and Raimondo, M. (2004), Wavelet deconvolution in a periodic setting. *J. Roy. Statist. Soc. Ser. B* **66**, 547–573.

Johnstone, I. M. and Silverman, B. W. (1990), Speed of estimation in positron emission tomography and related inverse problems. *Ann. Statist.* **18**, 251–280.

Kaipio, J.-P. and Somersalo, E. (2005), *Computational and Statistical Methods for Inverse Problems.* Springer-Verlag, New York.

Kallenberg, W. C. M. and Ledwina, T. (1995), Consistency and Monte Carlo simulation of a data driven version of smooth goodness-of-fit tests. *Ann. Statist.* **23**, 1594–1608.

Kress, R. (1999), *Linear Integral Equations.* 2nd edn. Springer, New York.

Ledwina, T. (1994), Data-driven version of Neyman's smooth test of fit. *J. Am. Statist. Assoc.* **89**, 1000–1005.

Loubes, J.-M. and Ludeña, C. (2004), Penalized estimators for nonlinear inverse problems. Preprint.

Mair, B. A. and Ruymgaart, F. H. (1996), Statistical inverse estimation in Hilbert scales, *SIAM J. Appl. Math.* **56**, 1424–1444.

Mallows, C.L. (1973). "Some comments on C_p", *Technometrics* **15**, 661–675.

Munk, A., Bissantz, N., Wagner, T. and Freitag, G. (2005), On difference based variance estimation in nonparametric regression when the covariate is high dimensional, *J. Roy. Statist. Soc. Ser. B* **67**, 19–41.

Natterer, F. (1986), *The Mathematics of Computerized Tomography.* B. G. Teubner, Stuttgart.

Neyman, J. (1937), 'Smooth' test for goodness of fit. *Skandinavisk Aktuarietidskrift* **20**, 149–199.

Nourrit, V., Vohnsen, B. and Artal, P. (2005), Blind deconvolution for high-resolution confocal scanning laser ophthalmoscopy, *J. Opt. A: Pure Appl. Opt.* **7**, 585–592.

Pepperkok, R. and Ellenberg, J. (2006), High-throughput fluorescence microscopy for systems biology. *Nat. Rev. Mol. Cell. Biol.* **9**, 690–696.

Petrov, V. (1995), *Sequences of Independent Random Variables*, Oxford University Press, Oxford.

Rice, J. (1984), Bandwidth choice for nonparametric regression, *Ann. Statist.* **12**, 1215–1230.

Schwarz, G. (1978), Estimating the dimension of a model. *Ann. Statist.* **6**, 461–464.

Spitzer, F. (1956), A combinatorial lemma and its applications to probability theory. *Trans. Am. Math. Soc.* **82**, 323–339.

Vardi, Y., Shepp, L. A. and Kaufman, L. (1985), A statistical model for positron emission tomography. *J. Am. Statist. Assoc.* **80**, 8–37.

Appendix

Proof of Lemma 1. Note that from (3), there are $c_1, C_1 > 0$ such that

$$c_1\big((m+p)^{2\beta+1} - p^{2\beta+1}\big) \le \Lambda_m \le C_1\big((m+p)^{2\beta+1} - p^{2\beta+1}\big).$$

Therefore, from the Hajek-Renyi inequality (cf. Petrov, 1995, p. 53) we have for $k \ge n$ and $x > 1$ that

$$\begin{aligned} P\Big(\max_{n\le m\le k} \frac{1}{\Lambda_m}\sum_{j=1}^{m}\frac{Z_j^2}{\lambda_{j+p}^2} \ge x\Big) &= P\Big(\max_{n\le m\le k} \frac{1}{\Lambda_m}\sum_{j=1}^{m}\frac{Z_j^2-1}{\lambda_{j+p}^2} \ge x-1\Big) \\ &\le \frac{1}{(x-1)^2}E(Z_1^2-1)^2\Big(\frac{1}{\Lambda_n^2}\sum_{j=1}^{n}\frac{1}{\lambda_{j+p}^4} + \sum_{j=n+1}^{k}\frac{1}{\Lambda_j^2\lambda_{j+p}^4}\Big) \\ &\le \frac{L}{(x-1)^2}\Big(\frac{1}{n^{4\beta+2}}\sum_{j=1}^{n} j^{4\beta} + \sum_{j=n+1}^{k}\frac{j^{4\beta}}{j^{4\beta+2}}\Big) \end{aligned}$$

for some $L > 0$. Letting $k \to \infty$ proves (9) as well as $P(T < \infty) = 1$. The statement $P(T \geq 1)$ will follow if we show that

$$\frac{1}{\Lambda_m} \sum_{j=1}^{m} \frac{Z_j^2}{\lambda_{j+p}^2} \to 1 \quad a.s., \quad m \to \infty.$$

To this end note that the conditions of Theorem 3 (ii), Chap. 3.3. in Chow and Teicher (1978) are satisfied for $a_j = 1/\lambda_{j+p}^2$, since $b_m = \Lambda_m / a_m \sim m$ evidently satisfies the conditions of their theorem. This concludes the proof of the lemma. □

Proof of Theorem 2. Since $\hat{\sigma}^2$ is consistent for σ^2, it will be sufficient to prove Theorem 2 for the case of known σ^2. We will show that $P(T_n > x) \to P(T > x)$ for $x > 1$. Let

$$S_{m,n} = \frac{1}{\Lambda_m} \sum_{j=1}^{m} \frac{n\, \hat{b}_{j+p,n}^2}{\sigma^2 \lambda_{j+p}^2}, \qquad S_m = \frac{1}{\Lambda_m} \sum_{j=1}^{m} \frac{Z_j^2}{\lambda_{j+p}^2}.$$

Then

$$|P(T_n > x) - P(T > x)| \leq P(A_n) + P(B_n) + |P(C_{n,1}) - P(C_{n,2})|,$$

where

$$\begin{aligned}
A_n &= \Big\{ S_m \leq x,\ 1 \leq m \leq m_n, \quad \sup_{m_n+1 \leq m < \infty} S_m > x \Big\}, \\
B_n &= \Big\{ S_{m,n} \leq x,\ 1 \leq m \leq m_n, \quad \max_{m_n+1 \leq m < n-p} S_{m,n} > x \Big\}, \\
C_{n,1} &= \Big\{ \max_{1 \leq m \leq m_n} S_m > x \Big\}, \quad C_{n,2} = \Big\{ \max_{1 \leq m \leq m_n} S_{m,n} > x \Big\},
\end{aligned}$$

where $m_n \to \infty$ is a sequence which will be specified below. From an application of the multivariate Berry-Esseen theorem (cf. Bhattacharya and Rango Rao, 1976) as in Eubank and Hart (1992) and Hart (1997), we get that

$$|P(C_{n,1}) - P(C_{n,2})| \leq a(m_n) m_n^2 \frac{E\epsilon_1^4}{\sigma^4 \sqrt{n}},$$

where $a(m)$ only depends on m. Thus it is possible to find a sequence $m_n \to \infty$ slowly enough such that

$$|P(C_{n,1}) - P(C_{n,2})| \to 0.$$

Furthermore, from Lemma 1 we immediately see that $P(A_n) \to 0$. Finally consider B_n. Let $Z_{j,n} = n\, \hat{b}_{j+p,n}^2 / \sigma^2$. We follow the proof in Eubank and Hart (1992). We have

$$B_n^c \supset \bigcap_{k=m_n+1}^{n-p} \left\{ \frac{\left| \sum_{j=1}^{k} (Z_{j,n}^2 - 1)/\lambda_{j+p}^2 \right|}{\Lambda_{k,p}} \leq x - 1 \right\}.$$

Let $n_j = j^2$, $j(1)$ largest integer j such that $j^2 \leq m_n$, and $j(2)$ largest integer j such that $j^2 < n - p$. Define

$$\begin{aligned}
\xi_{j,n} &= \max_{1 \leq r \leq n_{j+1} - n_j} \left| \sum_{i=n_j+1}^{n_j+r} \big(Z_{i,n}^2 - 1\big)/\lambda_{i+p}^2 \right|, \qquad j = j(1), \ldots, j(2) - 1, \\
\xi_{j(2),n} &= \max_{1 \leq r \leq n-1-n_{j(2)}} \left| \sum_{i=n_j+1}^{n_j+r} \big(Z_{i,n}^2 - 1\big)/\lambda_{i+p}^2 \right|.
\end{aligned}$$

For any integer k with $m_n + 1 \le k \le n$, either $n_j < k \le n_{j+1}$ for some $j(1) \le j \le j(2)$, or $n_{j(2)} < k \le n - p$. It follows that for $m_n + 1 \le k \le n - p$,

$$\frac{\left|\sum_{i=1}^{k}(Z_{i,n}^2 - 1)/\lambda_{i+p}^2\right|}{\Lambda_{k,p}} \le \frac{\left|\sum_{i=1}^{n_j}(Z_{i,n}^2 - 1)/\lambda_{i+p}^2\right|}{\Lambda_{n_j,p}} + \frac{\xi_{j,n}}{\Lambda_{n_j,p}}.$$

Hence

$$B_n^c \supset \bigcap_{j=j(1)}^{j(2)} \left[\left\{ \frac{\left|\sum_{i=1}^{n_j}(Z_{i,n}^2 - 1)/\lambda_{i+p}^2\right|}{\Lambda_{n_j,p}} \le \frac{x-1}{2} \right\} \bigcap \left\{ \frac{\xi_{j,n}}{\Lambda_{n_j,p}} \le \frac{x-1}{2} \right\} \right]. \tag{14}$$

From Markov's inequality,

$$P\left(\bigcup_{j=j(1)}^{j(2)} \left\{ \frac{\left|\sum_{i=1}^{n_j}(Z_{i,n}^2 - 1)/\lambda_{i+p}^2\right|}{\Lambda_{n_j,p}} > \frac{x-1}{2} \right\} \right) \le \frac{4}{(x-1)^2} \sum_{j=j(1)}^{j(2)} \frac{v(1,n_j,n)}{\Lambda_{n_j,p}^2}, \tag{15}$$

where for $s \le r$, by computing the variance of the quadratic form,

$$\begin{aligned} v(s,r,n) &= \mathrm{Var}\left[\sum_{i=s}^{r}(Z_{i,n}^2 - 1)/\lambda_{i+p}^2 \right] \\ &= \frac{1}{n^2\sigma^4} \left(\sum_{k=1}^{n} \left(\sum_{i=s}^{r} \psi_{i+p}^2(x_k)/\lambda_{i+p}^2 \right)^2 \right) \left(E\epsilon_1^4 - 3\sigma^4 \right) \\ &\quad + \frac{2}{n^2} \sum_{k,l=1}^{n} \left(\sum_{i=s}^{r} \psi_{i+p}(x_k)\psi_{i+p}(x_l)/\lambda_{i+p}^2 \right)^2 \\ &\le C \left(\Big(\sum_{i=s}^{r} \frac{1}{\lambda_{i+p}^2} \Big)^2 / n + \sum_{i=s}^{r} \frac{1}{\lambda_{i+p}^4} \right), \end{aligned} \tag{16}$$

where we used (6). Here and in the following $C > 0$ is a generic constant which might change from line to line. Using (3) one shows that the right-hand side of (15) is of order

$$\sum_{j=j(1)}^{j(2)} \frac{\left((j^2)^{2\beta+1}\right)^2/n + (j^2)^{4\beta+1}}{(j^2)^{4\beta+2}}, \tag{17}$$

which tends to 0 as $n, m_n \to \infty$.

Next we estimate the contribution of the second term in the intersection (14). Note that from (16), we get

$$v(s,r,n) \le C \sum_{i=s}^{r} \frac{1}{\lambda_{i+p}^4}.$$

Therefore we can use an inequality due to Billingsley (1968, p.102) with $\nu = 2$, $\alpha = 1$ and $u_i = \lambda_{i+p}^{-4}$ to estimate

$$E\xi_{j,n}^2 \le C \left(\log(8j+4) \right)^2 \sum_{i=n_j+1}^{n_{j+1}} \frac{1}{\lambda_{i+p}^4}$$

Thus

$$\begin{aligned} P\left(\bigcap_{j=j(1)}^{j(2)} \left\{ \frac{\xi_{j,n}}{\Lambda_{n_j,p}} \le \frac{x-1}{2} \right\} \right) &\ge 1 - \sum_{j=j(1)}^{j(2)} \left(\log(8j+4) \right)^2 \Lambda_{n_j,p}^{-2} \sum_{i=n_j+1}^{n_{j+1}} \frac{1}{\lambda_{i+p}^4} \\ &\ge 1 - C \sum_{j=j(1)}^{j(2)} j^{-2}, \end{aligned}$$

which tends to 1 as $m_n \to \infty$. This proves that $P(B_n) \to 0$, as desired. □

Proof of Theorem 3. From (11) and Lemma 1,

$$\begin{aligned} P\big(T_n \geq c_\alpha\big) &\geq P\Big(\frac{1}{\Lambda_j}\sum_{i=1}^{j}\frac{n\,\hat{b}^2_{i+p,n}}{\hat{\sigma}^2\lambda^2_{i+p}} \geq c_\alpha\Big) \\ &\geq P\Big(\hat{b}^2_{j+p,n} \geq \frac{\hat{\sigma}^2\lambda^2_{j+p}\Lambda_j c_\alpha}{n}\Big) \to 1. \end{aligned}$$

□

Proof of Theorem 4. Using (16) and Markov's inequality, for $k \geq 2$ we estimate

$$\begin{aligned} P\big(\tilde{k}=k\big) &\leq P\big(\sum_{j=1}^{k}\frac{n\hat{b}^2_{j+p,n}}{\sigma^2\lambda^2_{j+p}} - \Lambda_k\,\log n \geq \frac{n\hat{b}^2_{1+p,n}}{\sigma^2\lambda^2_{1+p}} - \Lambda_1\,\log n\big) \\ &= P\big(\sum_{j=2}^{k}\frac{Z^2_{j,n}-1}{\lambda^2_{j+p}} \geq (\Lambda_k-\Lambda_1)\,(\log n\ -1)\big) \\ &\leq C\left(\Big(\sum_{i=2}^{k}\frac{1}{\lambda^2_{i+p}}\Big)^2/n + \sum_{i=2}^{k}\frac{1}{\lambda^4_{i+p}}\right)\Big/\Big((\Lambda_k-\Lambda_1)\,(\log n\ -1)\Big)^2, \end{aligned}$$

which tends to 0 as $n \to \infty$. □